Available online at www.sciencedirect.com

ScienceDirect

Mendeleev Commun., 2021, **31**, 647–650

Mendeleev Communications

Fabrication of carbon quantum dots *via* ball milling and their application to bioimaging

Meng-Jey Youh,[a] Meng-Chih Chung,[b] Hung-Chun Tai,[b] Ching-Yi Chen[b] and Yuan-Yao Li*[b,c]

[a] *Department of Mechanical Engineering, Ming Chi University of Technology, 24301 New Taipei, Taiwan*
[b] *Department of Chemical Engineering, National Chung Cheng University, 62102 Chia-Yi, Taiwan. Fax: +886 5 2721206; e-mail: chmyyl@ccu.edu.tw*
[c] *Advanced Institute of Manufacturing with High-Tech Innovations, National Chung Cheng University, 62102 Chia-Yi, Taiwan*

DOI: 10.1016/j.mencom.2021.09.018

Carbon quantum dots (CQDs) with an average diameter of 3 nm, exhibiting blue photoluminescence, have been obtained from commercial conductive carbon black by a cost-effective and straightforward exfoliation method using dry ball milling in the presence of sodium carbonate. As a secondary abrasive medium, sodium carbonate provides effective exfoliation of carbon black with a high degree of CQD graphitization and plays an essential role in the functionalization of CQDs with oxygen groups. Due to the low toxicity of CQDs against HeLa cancer cells (cell viability above 90% at a CQD concentration of 200 μg cm^{-3}) and the ability to penetrate cells and emit blue light, CQDs are possibly suitable for biological imaging of cells.

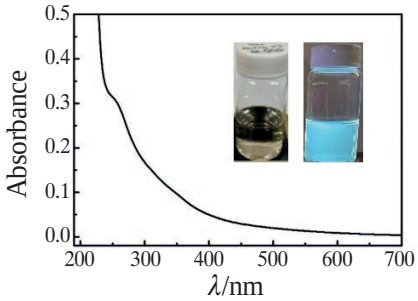

Keywords: carbon quantum dots, ball milling, conductive carbon black, sodium carbonate, bioimaging.

Carbon dots are an emerging material with several unique properties, including tunable fluorescence, low toxicity and excellent stability in aqueous media.[1] Carbon quantum dots (CQDs) are a type of carbon dots less than 10 nm in diameter.[2] CQDs are composed of sp^2 and sp^3 carbon atoms forming C=C and C–C bonds and have a structure similar to graphene and molecule-like characteristics[3] that give them good chemical stability and excellent biocompatibility.[4] CQDs can be used in various applications, including biological cell imaging,[5] drug delivery,[2] displays,[6] light sources,[6] solar cells[24,26] and sensors.[4]

The mechanism of CQD luminescence is associated with the quantum confinement effect[6] and the CQD surface state[7]. Due to the quantum confinement effect, the fluorescence characteristics of CQDs depend on the particle size; *i.e.*, the fluorescence wavelength decreases with decreasing particle size. The CQD surface structure (*e.g.*, carbon boundaries and surface defects) and composition (*e.g.*, dopants) affect the CQD energy gap and thus change the luminescence in terms of a fluorescence shift and phosphorescence.[8]

In general, CQD preparation methods can be divided into bottom-up and top-down methods. Bottom-up methods allow CQDs to be synthesized through chemical reactions, making them fast and straightforward. An example is a hydrothermal synthesis,[9] where the crystallization of monomers occurs at high temperature and vapor pressure. Top-down methods produce CQDs by reducing the size of carbon-based materials *via* a physical or chemical process. Examples include the acid oxidation method[10] and electrochemistry method.[11] Top-down methods often require strong acids or bases such as citric acid, ethylenediamine, nitric acid and dimethyl sulfite.[12,13] Waste from the production process can be an environmental problem. In addition, the processes are complex and energy-intensive.

Ball milling has recently become a method for preparing CQDs. In ball milling, the size of materials is reduced by grinding using ceramic or stainless steel balls as the abrasive medium. For the production of CQDs, an additional abrasive medium can be used during the ball milling process to increase grinding efficiency and stimulate chemical reactions. The media used were magnesium,[14] sodium chloride,[15] potassium hydroxide,[16] potassium carbonate[17] and sodium carbonate.[18] Various types of carbon-based materials, including activated carbon, graphite and cellulose,[16] can be used as carbon sources to fabricate CQDs. It is important to select a suitable carbon source with a small particle size to achieve efficient exfoliation and obtain good graphitic crystallinity to ensure high-quality CQDs.

In this paper, we demonstrate a simple and economical ball milling process for the production of CQDs using commercial carbon black as a carbon source and sodium carbonate as an abrasive and reaction medium. The abrasive media, namely sodium carbonate and zirconia balls, effectively exfoliate carbon black, while dry milling provides high impact and an attrition force for size reduction. Conductive carbon black (Ketjen, KJ, carbon black, diameter: 20–30 nm) is considered a good carbon source for CQDs formation due to its small particle size and good graphitic crystallinity. The prepared CQDs exhibit blue photoluminescence (PL) in ultraviolet (UV) light, hydrophilicity and low toxicity, suggesting that they can be used for cell imaging.

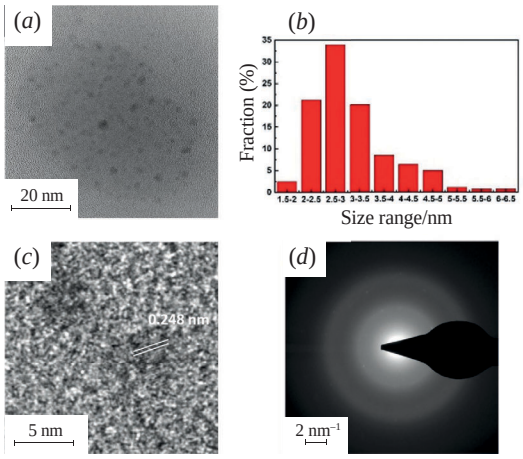

Figure 1 (*a*) TEM image, (*b*) particle size distribution, (*c*) high-resolution TEM image and (*d*) selected area electron diffraction pattern of the prepared CQDs.

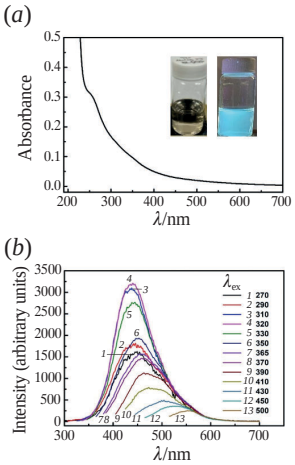

Figure 2 (*a*) UV-VIS spectrum of the CQD solution and its appearance under (left inset) visible and (right inset) UV light and (*b*) PL spectra of CQDs obtained at excitation wavelengths from 270 to 500 nm.

The experimental details are described in Online Supplementary Materials. Briefly, CQDs were fabricated as follows. The mixture of KJ carbon black, sodium carbonate (Na_2CO_3) and zirconia balls was dry ground in a planetary mill at the desired speed for the desired time. Deionized water was used to dissolve the CQDs in the mixture. The resulting dispersion was centrifuged, and the supernatant was filtered. The filtrate was dialyzed to remove ions. The processed dialysate (CQD solution) was freeze-dried to obtain the CQDs.

The SEM and TEM images of KJ carbon black (Figure S1, see Online Supplementary Materials) show that the carbon black particles have a graphitic structure with a short-range order and diameters in the 20–30 nm range. According to the TEM image of the produced CQDs [Figure 1(*a*)], they have an irregular shape and size distribution of 1.5–6.5 nm† with an average size of about 3 nm [Figure 1(*b*)]. The high-resolution TEM image [Figure 1(*c*)] reveals that the lattice spacing of 0.248 nm is close to the (1120) spacing in the graphite structure.[19] The ring-like selected area electron diffraction pattern [Figure 1(*d*)] indicates a plurality of CQD crystals with different orientations. Thus, the material is neither amorphous carbon dots nor single-crystal graphene quantum dots.[20]

The survey X-ray photoelectron spectrum (XPS) of the CQDs [Figure S2(*a*)] shows strong peaks at 284.5 eV (carbon) and 531.0 eV (oxygen). The C 1*s* spectrum of the CQDs [Figure S2(*b*)] displays four fitted peaks, namely C=C sp^2 (284.0 eV), C–C sp^3 (284.5 eV), C–O (286.0 eV) and COOH (288.5 eV).[21] The percentage distribution of the C=C, C–C, C–O and COOH bonds was 42.31, 27.40, 19.19 and 11.11%, respectively. The C 1*s* spectrum of KJ carbon black is shown in Figure S2(*c*) for comparison. The intensity ratio of C=C sp^2 to C–C sp^3 is 1.14 for KJ carbon black and 1.55 for the CQDs, indicating that the CQDs have a higher graphitization degree than KJ carbon black. The O 1*s* spectrum of the CQDs [Figure S2(*d*)] demonstrates a broad peak that can be fitted by two characteristic peaks, namely C=O (532 eV) and C–OH (533.5 eV).[8] There is no prominent peak in the O 1*s* spectrum for KJ carbon black [Figure S2(*e*)].

For comparison, experiments on grinding KJ carbon black in a ball mill were carried out without Na_2CO_3. The results show that only a minimal amount of CQDs is formed. The XPS spectra (Figure S3) show that without Na_2CO_3, fewer oxygen functional groups appear on the CQD surface. According to Raman [Figure S4(*a*)], Fourier transform infrared [Figure S4(*b*)] and XPS spectra of KJ carbon black and the CQDs, ball milling of KJ carbon black using zirconia beads and sodium carbonate as grinding media creates carbon/graphite nanofragments and changes the intrinsic and extrinsic properties. For example, the graphitization degree of the CQDs is higher than that of carbon black. All of this could have been the result of a high-energy impact during the ball milling process. In addition, a chemical reaction occurs since Na_2CO_3 in the ball milling process increases the amount of oxygen functional groups on the CQD surface, which increases the hydrophilicity of the CQDs. These results are in good agreement with those of the previous study.[22]

In the UV-VIS spectrum of CQDs [Figure 2(*a*)], an absorption peak at 257 nm is observed, consistent with another study.[23] CQDs emit blue light when irradiated with 365 nm light and yellow light when exposed to visible light [Figure 2(*a*), inset]. The CQDs disperse well in an aqueous solution; no sediments were found after six months. In the PL spectra of CQDs [Figure 2(*b*)], the intensity of the broad emission peak centered around 430 nm increases with increasing excitation wavelength (λ_{ex}) in the range from 280 to 320 nm. The peak intensity reaches a maximum at λ_{ex} = 320 nm. When λ_{ex} was increased to 390 nm or more, the CQDs exhibited PL behavior as a function of the excitation wavelength. The emission intensity dropped rapidly, and the emission peaks shifted to the red region. The redshift may be due to the oxidation of CQDs, the presence of oxygen-containing groups grafted to the CQDs and CQD size, which changes the energy gap of CQDs.[24]

The quantum yield of CQDs was calculated from UV-VIS spectra using quinine sulfate as a reference compound.[14] The quantum yield of CQDs was 2.23%, similar to the reported value for CQDs prepared using physical exfoliation methods.[25] The low quantum yield can be attributed to the relatively small amount of functional groups and defects in CQDs, which results in emission from an intrinsic state rather than from a defect state.[26] The yield of CQD production from raw KJ carbon black was about 6.9%. We believe that quantum yield, production yield and productivity can be increased, and size distribution can be narrowed by optimizing the milling process parameters (*e.g.*, carbon black/abrasive medium ratio and process time).

As shown above, the CQDs demonstrated good hydrophilicity and photostability. CQDs are environmentally friendly and relatively non-toxic, making them suitable for use as a cell imaging agent for visualizing biological systems, both *in vitro* and *in vivo*.[27] Here, the prepared CQDs were used to visualize HeLa cells. Figure 3(*a*) shows the results of the MTT assay of HeLa cell viability with various CQD concentrations. As shown, at a CQD concentration of up to 200 μg cm^{-3}, the viability of HeLa cells exceeds 90%, which means that the CQDs are

† TEM image was analyzed with ImageJ software.

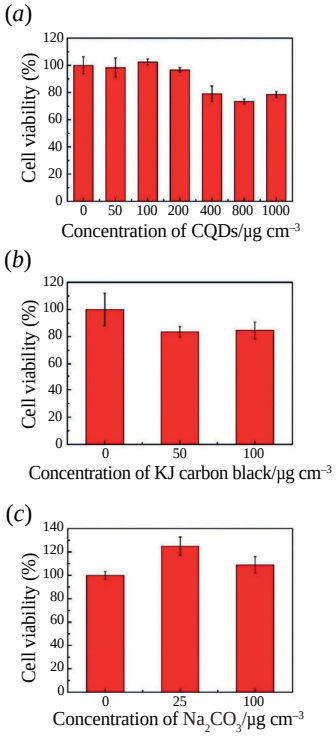

Figure 3 HeLa cell viability according to MTT assay with various concentrations of (*a*) CQDs (0, 50, 100, 200, 400, 800 and 1000 μg cm^{-3}), (*b*) KJ carbon black (0, 50 and 100 μg cm^{-3}) and (*c*) sodium carbonate (0, 25 and 100 μg cm^{-3}).

practically not cytotoxic to HeLa cells. Figures 3(*b*),(*c*) show the results of assays with KJ carbon black and Na_2CO_3 as controls. KJ carbon black reduced cell viability even at low concentrations. According to the visible-light images of HeLa cells [Figures 4(*a*),(*b*)], cell morphology is similar with and without CQDs. Upon excitation at a wavelength of 365 nm, blue fluorescence was observed from the cells in the presence of CQDs [Figure 4(*d*)], while no fluorescence was detected in the sample without CQDs [Figure 4(*c*)]. Blue fluorescence confirms that CQDs were taken up by HeLa cells. No decay in luminescence intensity was found even after a long excitation period, indicating that CQDs are a potential fluorescent probe for imaging living cells.

Regarding the mechanism for CQDs formation using the ball milling technique, we believe that sodium carbonate plays a significant role in increasing the grinding efficiency and functionalization of CQDs. During ball milling, much energy is transferred from the grinding beads to the target materials in the impact zone, and friction occurs between the fine particles in the abrasive zone. In the impact zone, the grinding beads crush the target materials (carbon black and Na_2CO_3), which leads to the disaggregation of the carbon black and the functionalization of the materials due to the high-energy impact. In the abrasive zone, the grinding beads force the materials to press against each other due to shear forces. Sodium carbonate particles act as an abrasive medium and filler between the grinding beads and carbon black, enhancing grinding efficiency. For the CQDs to form, the additional abrasive medium (*e.g.*, sodium carbonate) must be mechanically harder than the material (carbon) and less than the primary grinding beads.

In conclusion, a dry ball milling method was developed to produce CQDs using environmentally friendly and cost-effective KJ carbon black and sodium carbonate. The prepared CQDs have a narrow size distribution of 1.5–6.5 nm and an average size of 3.0 nm. The UV-VIS and PL spectra revealed that the maximum emission peak intensity was at 430 nm for an excitation wavelength of 320 nm and that the quantum yield was 2.23%. HeLa cells in a CQD solution showed good viability at CQD concentrations below 200 μg cm^{-3}, suggesting that CQDs are a promising material for bioimaging applications.

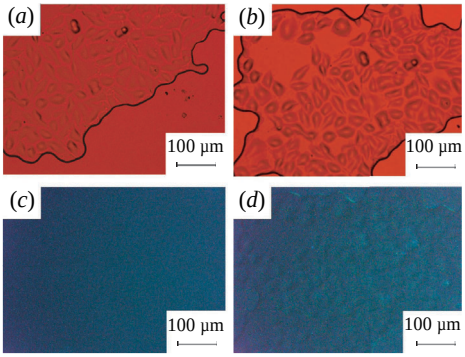

Figure 4 Microscopy images of HeLa cells obtained in visible light (bright field) (*a*) without and (*b*) with CQDs and with excitation at a wavelength of 365 nm (*c*) without and (*d*) with CQDs.

The authors would like to thank the Ministry of Science and Technology (MOST), Taiwan, for supporting this research under grant MOST 109-2221-E-194-015 and the Advanced Institute of Manufacturing with High-tech Innovations (AIM-HI) from The Featured Areas Research Center Program within the framework of the Higher Education Sprout Project by the Ministry of Education (MOE) in Taiwan.

Online Supplementary Materials

Supplementary data associated with this article can be found in the online version at doi: 10.1016/j.mencom.2021.09.018.

References

1 X. Xu, R. Ray, Y. Gu, H. J. Ploehn, L. Gearheart, K. Raker and W. A. Scrivens, *J. Am. Chem. Soc.*, 2004, **126**, 12736.
2 L. Xiao and H. Sun, *Nanoscale Horiz.*, 2018, **3**, 565.
3 M. Bacon, S. J. Bradley and T. Nann, *Part. Part. Syst. Charact.*, 2014, **31**, 415.
4 J. Shen, Y. Zhu, X. Yang and C. Li, *Chem. Commun.*, 2012, **48**, 3686.
5 H. Lu, W. Li, H. Dong and M. Wei, *Small*, 2019, **15**, 1902136.
6 Z. Gan, H. Xu and Y. Hao, *Nanoscale*, 2016, **8**, 7794.
7 H. Ding, S.-B. Yu, J.-S. Wei and H.-M. Xiong, *ACS Nano*, 2016, **10**, 484.
8 S. J. Bradley, R. Kroon, G. Laufersky, M. Röding, R. V. Goreham, T. Gschneidtner, K. Schroeder, K. Moth-Poulsen, M. Andersson and T. Nann, *Microchim. Acta*, 2017, **184**, 871.
9 D. Pan, J. Zhang, Z. Li and M. Wu, *Adv. Mater.*, 2010, **22**, 734.
10 R. Ye, C. Xiang, J. Lin, Z. Peng, K. Huang, Z. Yan, N. P. Cook, E. L. G. Samuel, C.-C. Hwang, G. Ruan, G. Ceriotti, A.-R. O. Raji, A. A. Martí and J. M. Tour, *Nat. Commun.*, 2013, **4**, 2943.
11 J. Lu, J. Yang, J. Wang, A. Lim, S. Wang and K. P. Loh, *ACS Nano*, 2009, **3**, 2367.
12 Y. Dong, C. Chen, X. Zheng, L. Gao, Z. Cui, H. Yang, C. Guo, Y. Chi and C. M. Li, *J. Mater. Chem.*, 2012, **22**, 8764.
13 D. Li, P. Jing, L. Sun, Y. An, X. Shan, X. Lu, D. Zhou, D. Han, D. Shen, Y. Zhai, S. Qu, R. Zbořil and A. L. Rogach, *Adv. Mater.*, 2018, **30**, 1705913.
14 Y. Han, Y. Chen, N. Wang and Z. He, *Mater. Technol.*, 2019, **34**, 336.
15 B. Alinejad and K. Mahmoodi, *Funct. Mater. Lett.*, 2017, **10**, 1750047.
16 L. Wang, X. Chen, Y. Lu, C. Liu and W. Yang, *Carbon*, 2015, **94**, 472.
17 L. Ge, G. Hu, B. Shi, Q. Guo, L. Li, L. Zhao and J. Li, *Appl. Phys. A: Mater. Sci. Process.*, 2019, **125**, 641.
18 M.-J. Youh, M.-Y. Jiang, M.-C. Chung, H.-C. Tai and Y.-Y. Li, *Inorg. Chem. Commun.*, 2020, **119**, 108061.
19 J.-S. Lin, Y.-W. Tsai, K. Dehvari, C.-C. Huang and J.-Y. Chang, *Nanoscale*, 2019, **11**, 20917.
20 M. Li, T. Chen, J. J. Gooding and J. Liu, *ACS Sensors*, 2019, **4**, 1732.
21 S. Kang, K. M. Kim, K. Jung, Y. Son, S. Mhin, J. H. Ryu, K. B. Shim, B. Lee, H. Han and T. Song, *Sci. Rep.*, 2019, **9**, 4101.

22 T. Xing, T. Ramireddy, L. H. Li, D. Gunzelmann, H. Zeng, W. Qi, S. Zhou and Y. Chen, *Phys. Chem. Chem. Phys.*, 2015, **17**, 5084.
23 B. Han, M. Yu, T. Pen, Y. Li, X. Hu, R. Xiang, X. Hou and G. He, *New J. Chem.*, 2017, **41**, 5267.
24 S. Hu, Z. Wei, Q. Chang, A. Trinchi and J. Yang, *Appl. Surf. Sci.*, 2016, **378**, 402.
25 L. Lu, Y. Zhu, C. Shi and Y. T. Pei, *Carbon*, 2016, **109**, 373.
26 S. Zhu, X. Zhao, Y. Song, B. Li, J. Zhang and B. Yang, in *Graphene Science Handbook: Mechanical and Chemical Properties*, eds. M. Aliofkhazraei, N. Ali, W. I. Milne, C. S. Ozkan, S. Mitura and J. L. Gervasoni, CRC Press, Boca Raton, 2016, pp. 163–178.
27 P. Gao, J. Wang, M. Zheng and Z. Xie, *Chem. Eng. J.*, 2020, **381**, 122665.

Received: 9th April 2021; Com. 21/6518